

Geomorphic Indices Characterization Related to Geothermal Manifestation Appearance in Cubadak Area, Pasaman Regency, West Sumatra Province

Amira Rahmah Azizah¹, Nana Sulaksana¹, Dewi Gentana¹

¹Geological Engineering Faculty, Padjadjaran University, Jatinangor, Indonesia

Email address: amira17001(at)mail.unpad.ac.id

Abstract— Indonesia has 351 spots of geothermal potential area with installed electric power is about 8.9% of total energy. Sumatra Island has 101 geothermal potential spots with energy total is 9,679 MW. One of potential areas in Sumatra Island is located in Cubadak Geothermal Area, Pasaman Regency, West Sumatra Province which indicated by surface manifestation of hot springs and have 70 MWe estimated potential (Ditjen EBTKE, 2017). This research aimed to determine the correlation between geomorphic indices to the distribution of surface geothermal manifestation. The research method analyzed the geological lineament and calculate geomorphic indices through SRTM- DEM image and SHP data; lineament density (Ld), mount-front sinuosity (Smf), bifurcation ratio (Rb), valley floor width – valley height ratio (Vf) and drainage density (Dd). Geological lineament that interpreted as geological structure has main pattern northwest - southeast (NW - SE) orientation. The calculation of geomorphic indices results Ld value; 0.000 – 1.501 Km⁻¹ (low – high), Smf value; 1.0 – 3.2 (moderate – active tectonic), Vf value; 0.14 – 0.47 (high uplift tectonic), Rb value in general; 3.26 – 4.56 (not deformed area), and formed rough – very fine landform texture of Dd value; 2.58 – 7.29 Km⁻¹, related to surface manifestation distribution; AR1 group on A6 and A15 sub-watershed, AR2 on A15 sub-watershed and AR3 on A2 sub-watershed (Pasaman watershed).

Keywords— Geological Lineament Geomorphic Indices, Hot Spring Manifestation.

I. INTRODUCTION

Energy used in Indonesia was 5,355,006 Terajoules on 2019, increase for ± 9% compared to 2018 with energy use 4,947,693 Terajoules (Badan Pusat Statistik, 2020). The main energy providers on 2018 and 2019 were dominated by fossil fuels especially coal and oil (Adiarso et al., 2020; Badan Pusat Statistik, 2020). Renewable energy is needed to replace the fossil energy use, one of renewable energies is geothermal that associated with presence of volcanoes. Indonesia has very large geothermal energy potential because it is located on Pacific Ring of Fire and has 127 volcanoes include A, B and C type of volcanoes (PVMBG, 2017). Indonesia has 351 geothermal resource locations with total power 23,965.5 MW. Installed capacity of electrical energy on 2019 that derived from geothermal energy was 2,130.7 MW about 8.9% of the total geothermal resources (Ditjen EBTKE, 2020).

Cubadak geothermal area has hot spring as surface manifestation and preliminary research show 70 – 100 MW energy potential (Ditjen EBTKE, 2017; Nurhadi et al., 2009). Administratively the research area located on Pasaman Regency, West Sumatra Province, Indonesia (Fig. 1). The

appearance of surface manifestation in Cubadak area associated with geological structure due to tectonic activity and then act as a path flow for sub-surface heated fluid to flow to the surface (Nurhadi et al., 2009). Cubadak geothermal potential is influenced by Sumatra tectonic and Talamau Mount activity (Utami et al., 2018). Tectonic activity level can be studied through geomorphic indices characterization, analyzed from morphometry and morphotectonic also can be related to the appearance of geothermal surface manifestation (Gentana, 2018).

II. METHOD

The object of this research is tectonic activity level, geological lineament (ridge and valley) interpreted as fault, watershed and location of surface manifestation. This research conducted by geospatial analysis (remote sensing) using shapefile (SHP) and Shuttle Radar Topography Mission – Digital Elevation Model (SRTM-DEM) data. The tectonic activity level analysis using five of geomorphic indices are; lineament density (Ld), mount front sinuosity (Smf), bifurcation ratio (Rb), valley floor width – valley height ratio (Vf), and drainage density (Dd). The result of geomorphic indices analysis will be correlated to the appearance of surface manifestation.

A. Lineament Density (Ld)

Lineament density is defined as the total length of lineament (Km) in each one-unit area (Km²) (Soengkono, 1999). Lineament density analysis is aimed to find out an area that has a lot of fractures or faults that associated with the permeability zone. Lineament density value will be proportional with the permeability level, which is high lineament density also indicates a high permeable zone. Geothermal permeable zone can be associated with sub-surface fluid or reservoir (Gentana, 2018). Ld calculation using the equation (1) (Soengkono, 1999):

$$Ld = F/A \tag{1}$$

F : Lineament Frequency (Km)

A : Area calculation (Km²)

B. Bifurcation Ratio (Rb)

The calculation for river branching segment used Strahler (1952) method. Bifurcation ratio is the ratio between a certain river order (N_u) with the higher river order (N_{u+1}).

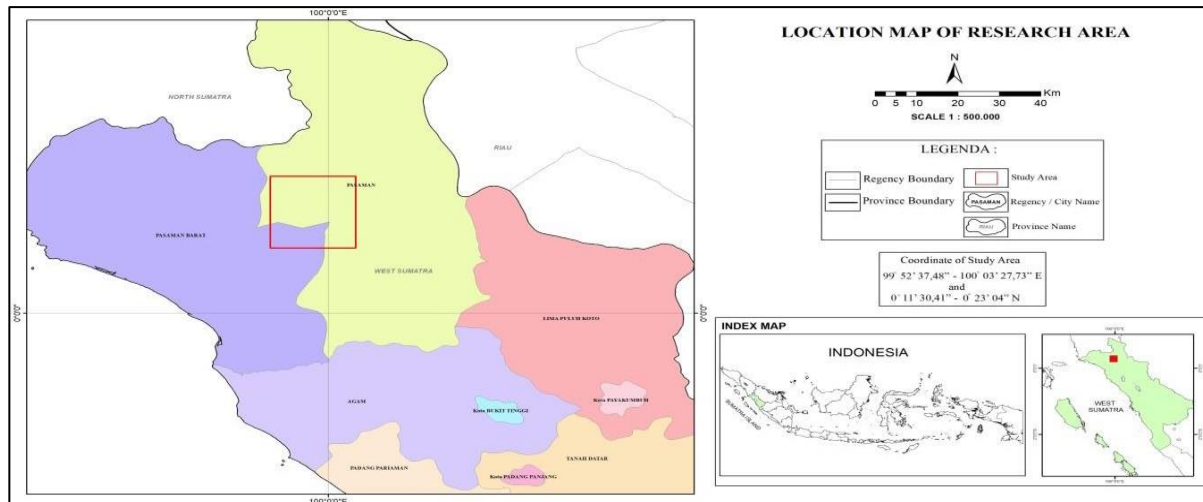


Fig 1. Research area located on Pasaman regency, West Sumatra province, Indonesia.

Rb analysis using the equation (2) (Horton, 1945; Gentana, 2018):

$$R_b = N_u / N_{u+1} \tag{2}$$

N_u : number of certain order

N_{u+1} : number of one higher order

The value $R_b < 1$ or $R_b > 5$ show a heterogeneous geological area and deformation occurred, while R_b value for 3-5 indicated not deformed area or tectonic activity not affected the river pattern (Verstappen, 1983; Gentana, 2018)

C. Valley Floor Width – Valley Height Ratio (Vf)

The calculation of valley floor width – valley height ratio is associated with uplift tectonic rate (Dehbozorgi, 2010; Gentana, 2018). Vf analysis using the equation (3) (Keller dan Pinter, 1996):

$$V_f = 2V_{f_w} / [(E_{ld} - E_{sc}) + (E_{rd} - E_{sc})] \tag{3}$$

V_{f_w} : Valley floor width

E_{ld} : elevation of left valley

top E_{rd} : elevation of right valley

top E_{sc} : Elevation of valley floor

Uplift rate is related with incision process where high uplift and high incision associated with low Vf value and the river stream will cut off the valley deeper or forms V-shape valley. Commonly the U-shaped valley has high Vf value with low uplift rate and then the river stream will cut off the valley wider (El Hamdouni, 2008; Keller dan Pinter, 1996). The Vf value for less than 0.5 indicated a high uplift rate. while more than 1.0 indicated a low uplift rate. Vf value for 0.5 – 1.0 indicated a moderate uplift rate (Keller dan Pinter. 1996; Gentana, 2018).

D. Mount Front Sinuosity (Smf)

Mount front sinuosity show the erosion process level to the mount front cutting, and active tectonic will results a straight mount front with active fault boundary (Keller dan Pinter, 1996). An active tectonic and uplift is associated with straight mount front and low value of Smf (El Hamdouni, 2008). Low value of Smf is dominated by uplift activity than erosion. Decreasing of uplift rate will enhanced the erosion process and then forms an irregular mount front and higher value of Smf (Perez-Pena, 2010; Keller dan Pinter, 1996). Smf calculation

use the equation (4) (Keller dan Pinter, 1996):

$$S_{mf} = L_{mf} / L_s \tag{4}$$

L_{mf} : length of mountain front segment

L_s : length of projected mountain front segment

S_{mf} value 1.2 – 1.6 show an active tectonic, S_{mf} ; 1.8 – 3.4 show a weak active tectonic and S_{mf} ; 2.0 – 5.0 show not active tectonic (Doornkamp, 1986; Gentana, 2018).

E. Drainage Density (Dd)

Drainage density calculated by divided the total length of river stream with the total of watershed or sub-watershed area (Nugroho et al., 2020). Drainage density related to the geological condition and climate, show the potential of surface run off, vegetation and surface relief. A low drainage density value associated with rough stream pattern while high value of drainage density associated with smooth stream pattern (Gentana, 2018). Drainage density calculation use the equation (5) (Horton, 1945; Gentana, 2018):

$$D_d = \sum L / A \tag{5}$$

$\sum L$: Total of river length segment (Km)

A : Watershed or sub-watershed area (Km²)

A high drainage density value reflects the high surfacewater flow. Tectonic control also affected rock deformation and forms a weak or fracture rock, then eroded by the surface water flow to form a river stream (Sukiyah, 2017). An area that has weak lithology or eroded easily indicated an occurring of tectonic deformation and forms higher drainage density value than a stable tectonic area (Sukiyah, 2012). A high drainage density value can show a sub-surface impermeable layer (Nugraha and Cahyadi, 2012). The value of Dd calculation divided into six class of landform texture (Sukiyah, 2009; Sukiyah, 2017) are very rough (Dd; 0.00 – 1.37 Km⁻¹), rough (Dd; 1.38 – 2.75 Km⁻¹), moderate (Dd; 2.76 – 4.13 Km⁻¹), rather smooth (Dd; 4.14 – 5.51 Km⁻¹), smooth (Dd; 5.52 – 6.89 m⁻¹) and very smooth (Dd; 6.90 – 8.27 Km⁻¹).

III. RESULT AND DISCUSSION

A. Regional Research Area

Sumatra Island divided into three parts based on the landscape (Badan Informasi Geospasial, 2015), there are North,

Central and South of Sumatra. The central part has thirteen landscape units, generally in mountain, hills and plain form. The research area located on Structural Hills of Bukit Barisan path unit.

The main physiography of Sumatra Island is characterized by the Ridge of Bukit Barisan with a northwest - southeast orientation (NW-SE) and the existence of a Semangko-rift Zone or known as Semangko Fault (Bemmelen, 1949). This fault generates several major depressions are Aceh Valley, Tangse, Alas, Angkola Gadis, Sumpur – Rokan Kiri, Solok – Singkarak, Muaralabuh, Kerinci, Ketahun, Kepahian – Makaukau and Semangko Valley (Katili and Hehuwat, 1967; Poedjoprajitno, 2007). Based on regional structure the research area located around the Sumpur – Rokan Kiri Valley (Fig. 2).

Based on the regional geologic, Cubadak area is a part of Lubuksikaping Regional Geology Map sheet (Rock et al., 1983). On regional geologic map show that Cubadak area has northwest – southeast (NW – SE) oriented structure, associated with Sumatra regional geologic structure. The research area is covered by eight rock units (Fig 3) are Alluvium (Qh), Undifferentiated Volcanic Product (Tmv), Ulai Intrusion (Tmiu), Undifferentiated Paleozoic and/or Mesozoic Limestone (Mpu), Pasaman Ultramafic Complex (Mupu), Panti Volcanic Formation (Ppvp), Silungkang Formation (Ppsl) and Kuantan Formation (Puku) Hot spring is come out on four locations are

in Tmv unit (Miocene volcanic tuff), and three locations of hot springs in Qh unit (Holocene alluvium rocks; sand, silt and gravel)

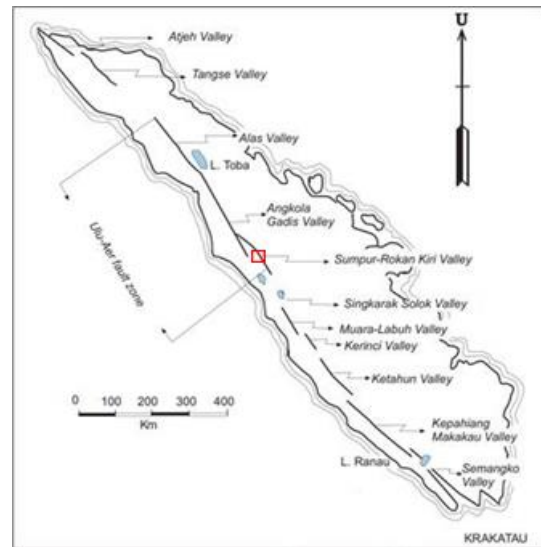


Fig 2. Research area located around Sumpur-Rokan Kiri Valley which includes in Ulu-Aer fault zone.

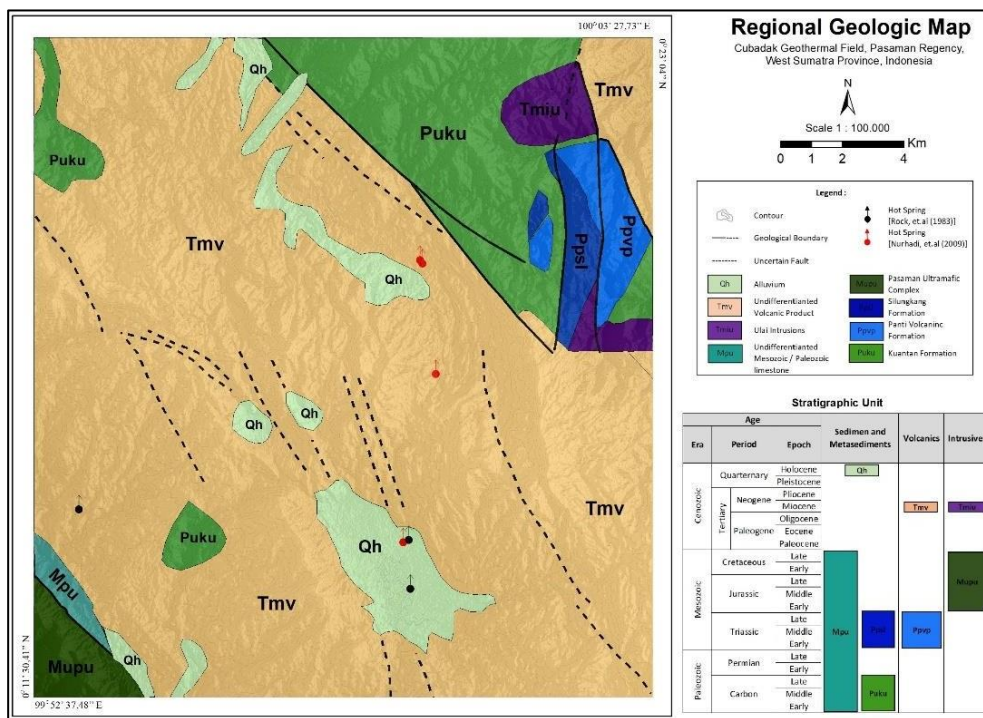


Fig 3. Lubuksikaping Regional Geologic Map sheet (modified from Rock et al., 1983), is location of research area.

B. Geothermal Manifestation of Research Area

The research area has hot springs as the surface manifestation on seven locations (Fig 4). Three of hot springs located on the central research area and one is located on the south that marked with red color (Nurhadi et al., 2009). Two

of hot springs located on south area and the last one is located on the southwest that marked with blue color (Rock et al., 1983). Based on previous research, the hot spring locations are grouped into three groups are Cubadak, Sawah Mudik and Talu (Nurhadi et al., 2009).

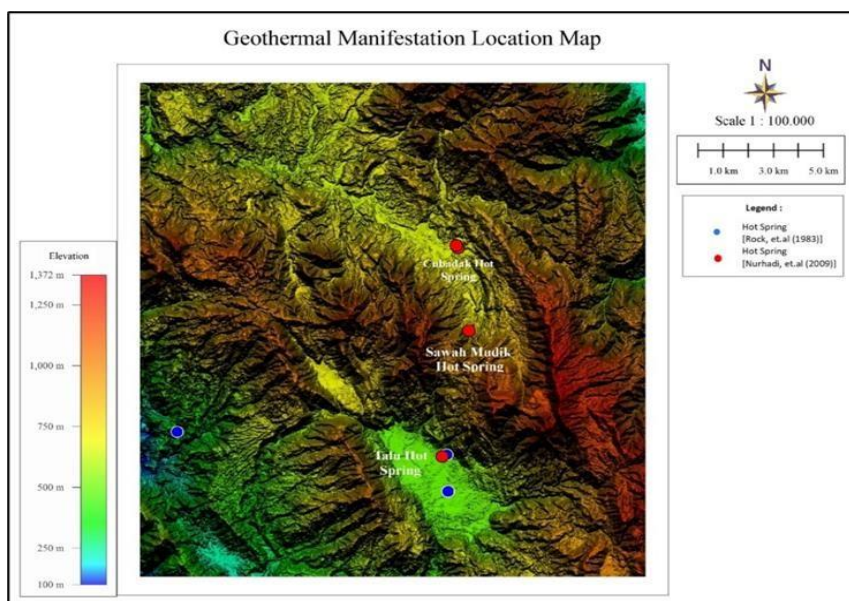


Fig 4. Geothermal manifestation location map shows the distribution of seven hot spring locations.

Cubadak hot spring has chloride - bicarbonate water type in partial equilibrium – immature water state, while Sawah Mudik hot spring has bicarbonate water type with immature water state (Nurhadi et al., 2009). Talu hot spring show bicarbonate water type with immature water state (Joni and Rahadinata, 2017). Na-K Fournier (1979) and Giggenbach (1988) geothermometer calculation show estimated reservoir temperature of Cubadak; 180.7 °C – 258.9°C. Sawah Mudik; 191.7 °C – 208.7 °C and Talu 187.2°C – 271.5°C (Utami et al.,2018). In addition, geophysics study found alteration zone

around Cubadak area in 100 – 500 m depth and around Sawah Mudik area in 100 – 750 m depth (Syahwanti et al., 2016).

C. Watershed and Sub-Watershed Delineation

Research area is located in part of Pasaman and Rokan watershed (RTRW, 2009). This research delineated the watershed (Fig 5) into twenty-two sub-watersheds and named by A1 to A22. Pasaman watershed delineated into twenty sub-watersheds and Rokan watershed is delineated into two sub-watersheds.

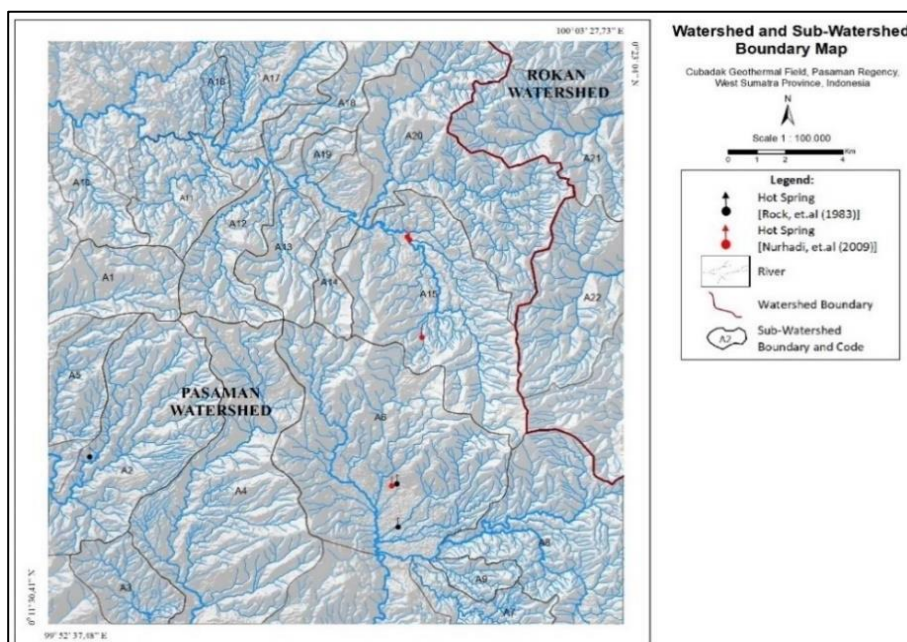


Fig 5. Research area located in Pasaman and Rokan watershed, delineated into twenty-two sub-watersheds.

D. Geological Lineament Pattern

Analysis show two lineament orientation patterns are northwest – southeast (NW – SE) and northeast – southwest (NE – SW). Ridge and valley lineament definitely has northwest – southeast (NW – SE) orientation showed on northeast area as a part of Panyabungan fault segment (normal fault) where the block on northeast side is relatively moving down (Soetoyo, 2008). On southern of research area show a circular (oval) high morphology with northwest – southeast orientation that interpreted as rim caldera. Inside of rim caldera formed a depression with broad and flat morphology (Fig 6). Based on morphogenetic this area was a volcanoes origin of Talu Mount crater remnant (Lumbanbatu, 2009).

Manifestation of research area found in two groups, the first is located on northern area with two locations of hot spring on a depression area as a moving down block of Panyabungan fault segment. The second group is located on southern area with three locations of hot spring in depression area as Mount Talu crater remnant. The appearance of first group is located on Holocene surface deposits (Nurhadi et al., 2009) while the second is located on Quarter sediment and metasediment rocks (Rock et al., 1983).

E. Geomorphic Index: Lineament Density (Ld)

Lineament density in research area has value ranging between 0 – 1.510 Km⁻¹, classified into three groups are low, moderate and high class (Fig 7). The low class has value ranging from 0 – 0.468 Km⁻¹, moderate class ranging between 0.468 – 0.806 Km⁻¹ and high class ranging between 0.806 – 1.510 Km⁻¹. The dark green color area dominated widely and circular on the central and northern research area as a depression morphology that illustrated in lineament map.

The hot spring appears on area with low lineament class for five location and moderate lineament class for two locations. The appearance of hot springs that dominated in low lineament class (low permeability rock) as anomaly may

occurred because the high lineament class is located on the higher elevation or high-rise area, while theoretically the hot spring will appear on normal fault or low part of an area. This is accordance with the five locations of hot spring in depression area (low lineament class), while two of hot springs appearance is associated with high intensity of fracture or fault (moderate lineament class).

F. Geomorphic Index: Mount Front Sinuosity (Smf)

Mount front sinuosity analysis on eighteen segments with various Smf value also Lmf and Ls length showed in Table 1. The Smf calculation show that research area has Smf value ranging between 1.0 – 3.2 classified as active and moderate active tectonic based on Doornkamp (1986) classification; the active tectonic are in eleven segments with Smf value; 1.1 – 1.6 and moderate are in seven segments with Smf value; 1.9 – 3.2. The hot spring located within segment number 3, 8, 9, 10, 14, 16 and 18 (Table 1 and Fig 8).

TABLE 1. Mount Front Sinuosity (Smf) calculation results in research area.

Mount Front Segment	Lmf (m)	Ls (m)	Smf	Tectonic Activity
1	11872	3722	3.2	Moderate
2	5467	3507	1.6	Active
3	5766	3641	1.6	Active
4	4977	4383	1.1	Active
5	7246	3411	2.1	Moderate
6	4022	2742	1.5	Active
7	5120	2474	2.1	Moderate
8	3408	2728	1.2	Active
9	5968	3736	1.6	Active
10	5757	3734	1.5	Active
11	5920	3179	1.9	Moderate
12	5891	2697	2.2	Moderate
13	4071	4013	1.0	Active
14	13388	6107	2.2	Moderate
15	4109	3373	1.2	Active
16	6423	4777	1.3	Active
17	14419	5331	2.7	Moderate
18	6332	4013	1.6	Active

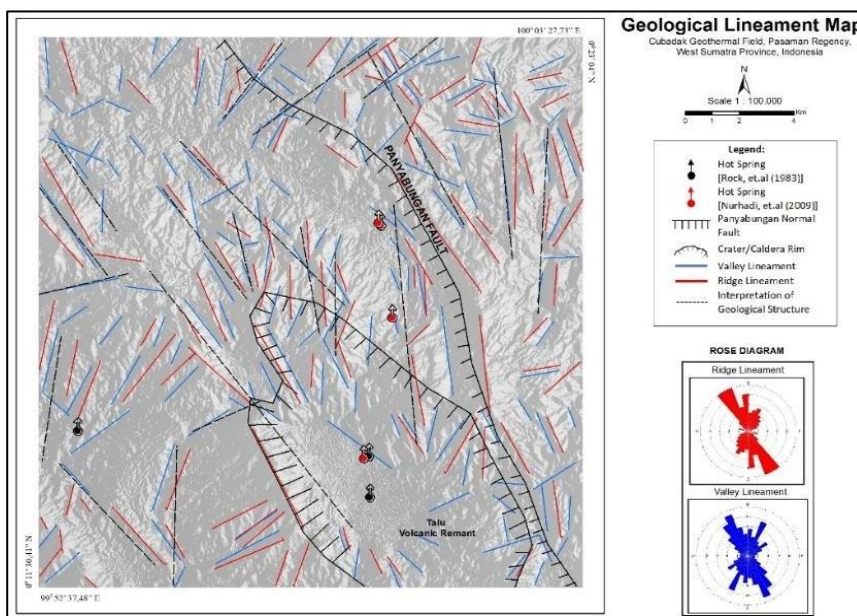


Fig 6. Ridge and valley lineament map show main lineament pattern is northwest – southeast (NW - SE) orientation.

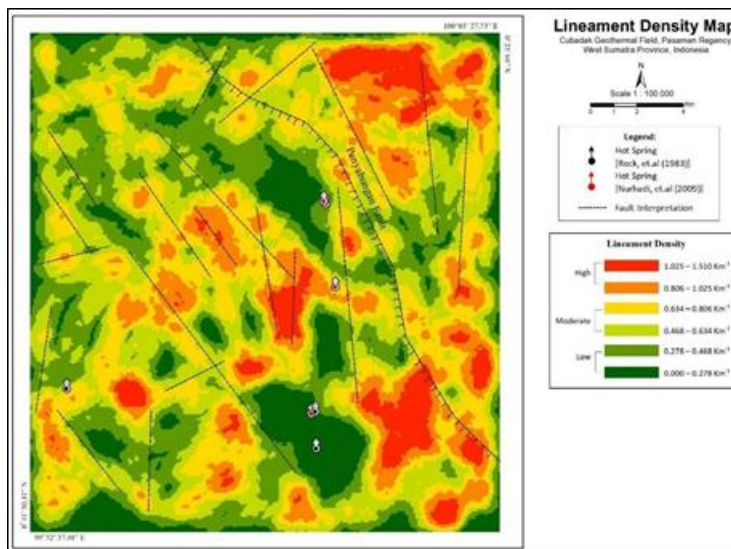


Fig 7. Lineament density map (Ld) map show research area has low – high lineament density value with range 0.000 – 1.510 Km⁻¹. Manifestations located on areawith Ld value; 0.000 – 0.806 Km⁻¹ (low – moderate).

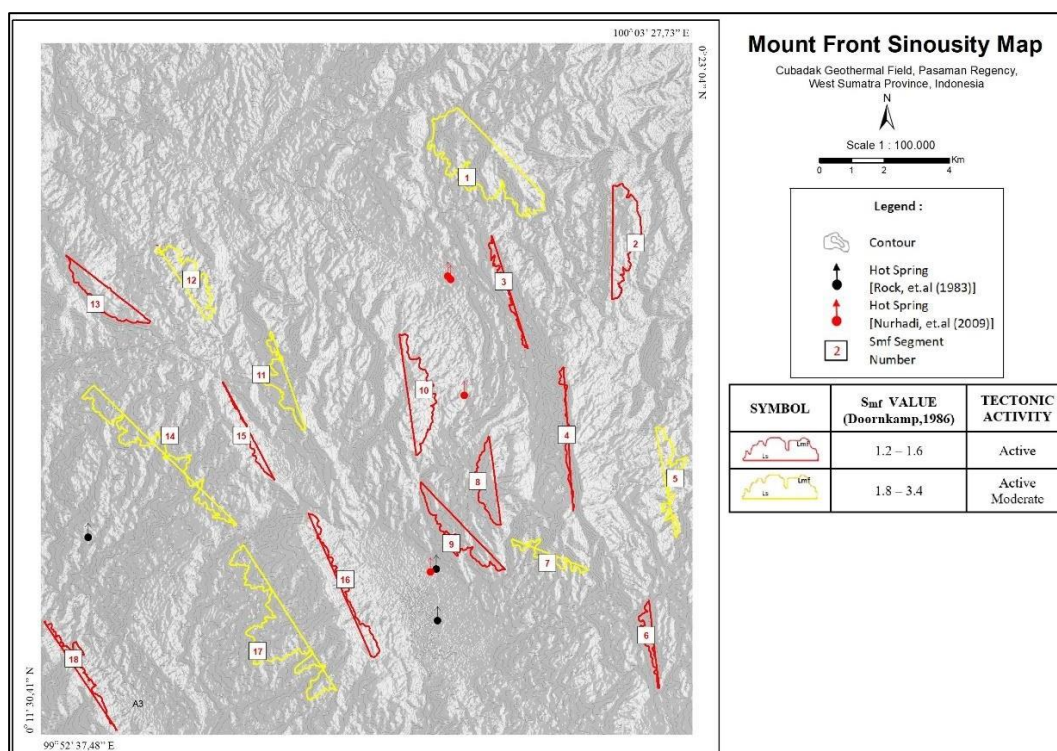


Fig 8. Sinuosity Mount Front (Smf) map show two class of tectonic activities are active and active moderate.

The appearance of hot spring is; two hot springs around segment-3 (active tectonic), one hot spring around segment-10 (active tectonic), three hot springs around segment-9 with (active tectonic) and one of hot spring on western area located between segment-14 (moderate active tectonic) and segment-18 (active tectonic). In generally, six of hot springs on eastern area appears around active tectonic segment (3, 9, 10 and 16), while one of hot springs on western area appears between moderate active and active tectonic segment (14 and 18). It is show that the appearance of hot springs in Cubadak is strongly influenced by tectonic activity based on mount front sinuosity analysis.

G. Geomorphic Index: Bifurcation Ratio (Rb)

Bifurcation ratio analysis using Strahler (1952) method for order numbering. Analysis result show that resarch area has river branching level (order) within 1st to 6th, but dominated by 4th or 5th river branching level (Table 2). Rb value are ranging between 3.26 – 6.92 and showed two indications of tectonic are deformed and not deformed area. Deformed sub-watershed located in A9 (Rb; 6.92) and A10 (Rb; 6.63) while not deformed sub-watershed is dominated with value ranging between 3.26 – 4.56.

TABLE 2. Bifurcation Ratio (Rb) analysis results in research area.

Sub-watershed	Segment Number of Stream Order						Rb Value					Tectonic Indication	
	1 st	2 nd	3 rd	4 th	5 th	6 th	1-2	2-3	3-4	4-5	5-6		Average Value
A1	42	9	2	1			4.67	4.50	2			3.72	Not Deformed
A2	170	36	11	3	1		4.72	3.27	3.67	3.00		3.67	Not Deformed
A3	53	15	3	1			3.53	5.00	3.00			3.84	Not Deformed
A4	149	38	6	2	1		3.92	6.33	3.00	2.00		3.81	Not Deformed
A5	70	12	3	1			5.83	4.00	3.00			4.28	Not Deformed
A6	201	41	13	3	1		4.90	3.15	4.33	3.00		3.85	Not Deformed
A7	88	22	6	1			4.00	3.67	6.00			4.56	Not Deformed
A8	312	66	16	4	2	1	4.73	4.13	4.00	2.00	2	3.37	Not Deformed
A9	47	6	1				7.83	6.00				6.92	Deformed
A10	42	8	1				5.25	8.00				6.63	Deformed
A11	82	19	5	1			4.32	3.80	5.00			4.37	Not Deformed
A12	53	12	4	1			4.42	3.00	4.00			3.81	Not Deformed
A13	33	8	3	1			4.13	2.67	3.00			3.26	Not Deformed
A14	13	5	1				2.60	5.00				3.80	Not Deformed
A15	159	43	14	5	1		3.70	3.07	2.80	5.00		3.64	Not Deformed
A16	51	10	2	1			5.10	5.00	2.00			4.03	Not Deformed
A17	158	36	7	3	1		4.39	5.14	2.33			3.96	Not Deformed
A18	49	12	4	1			4.08	3.00	4.00			3.69	Not Deformed
A19	13	4	1				3.25	4.00				3.63	Not Deformed
A20	268	56	12	2	1		4.79	4.67	6.00	2.00		4.36	Not Deformed
A21	114	24	7	2	1		4.75	3.43	3.50	2.00		3.42	Not Deformed
A22	136	29	6	2	1		4.69	4.83	3.00	2.00	5-6	3.63	Not Deformed

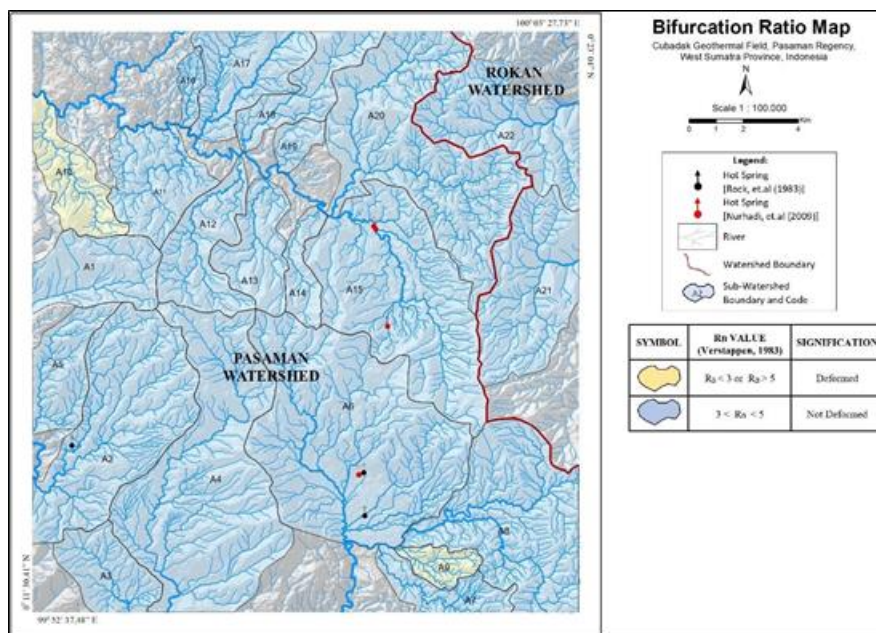


Fig 9. Bifurcation Ratio (Rb) map show in generally the research area has not deformed area (sub-watershed).

Hot spring manifestation appears on A2, A6 dan A15 sub-watershed in Pasaman watershed (Fig.9) also on not deformed area (generally associated with not active tectonic). The appearance of hot springs is; one hot spring on A2 sub-watershed (Rb; 3.67), three hot springs on A6 sub-watershed (Rb; 3.85) and three hot springs on A15 sub-watershed (Rb; 3.64). Hot spring appearance on not deformed area as anomaly may occur by others geological factor such as alteration rock or weathering that affect the rocks tend to be weak and low carrying capacity, so the rocks is eroded easily and forms depression landscape instead of hills or scarp as positive morphological (Gentana, 2018).

H. Geomorphic Index: Valley Floor Width – Valley Height Ratio (Vf)

This research analyzed 187 Vf segment and average value results ranging between 0.14 – 0.47 which is all of research area has a high uplift rate. The lowest Vf average value is

0.14 on A22 sub-watershed in Rokan watershed, meanwhile the A15 sub-watershed located on area that arranged of alluvium and sediment lake deposit Quarter rock unit (Nurhadi et al., 2009). A2 sub-watershed located on area arranged of volcanic Tertiary rocks unit, and A6 sub-watershed arranged by two type of rock unit while the hot spring located on sediment and metasediment Quarter rock unit (Rock et al., 1983). Based on Vf analysis the appearance of hot spring is controlled by high uplift tectonic rate highest Vf mean value is 0.47 on A19 sub-watershed in Pasaman watershed (Table 3).

TABLE 3. Bifurcation Ratio (Rb) analysis results in research area.

Segment	Vfw (m)	Esc (m)	Eld (m)	Erd (m)	Vf	Vf Value Mean	Tectonic Class
PASAMAN WATERSHED							
A1							
1.1	62.09	901.90	960.06	1035.53	0.65	0.37	High uplift rate
1.2	18.29	685.42	781.28	784.04	0.19		
1.3	20.80	889.44	959.03	971.26	0.27		
A2							
2.1	20.80	145.15	209.23	298.24	0.19	0.20	High uplift rate
2.2	16.74	269.29	378.20	365.04	0.16		
2.3	16.63	676.17	781.87	758.44	0.18		
2.4	21.55	537.23	630.09	609.04	0.26		
2.5	22.78	767.37	873.67	906.59	0.19		
A3							
3.1	10.75	273.92	324.44	321.07	0.22	0.30	High uplift rate
3.2	8.87	361.71	390.65	393.69	0.29		
3.3	11.40	325.15	347.22	361.41	0.39		
A4							
4.1	14.86	345.93	407.80	409.67	0.24	0.25	High uplift rate
4.2	18.38	650.56	792.99	741.95	0.16		
4.3	32.08	461.94	566.24	577.61	0.29		
4.4	27.45	587.46	764.76	786.40	0.15		
4.5	18.90	680.80	768.18	727.84	0.28		
4.6	50.94	749.83	1006.70	864.05	0.27		
4.7	15.56	362.13	397.76	410.59	0.37		
A5							
5.1	17.15	337.35	437.27	440.11	0.17	0.29	High uplift rate
5.2	31.31	397.97	429.52	467.60	0.62		
5.3	13.04	674.93	720.37	767.95	0.19		
5.4	17.28	234.99	304.93	338.50	0.20		
A6							
6.1	17.88	789.14	868.30	853.42	0.25	0.19	High uplift rate
6.2	14.00	760.24	850.43	892.58	0.13		
6.3	26.56	621.15	702.37	780.37	0.22		
6.4	21.00	987.49	1073.30	1192.11	0.14		
6.5	22.86	868.47	1015.19	962.62	0.19		
6.6	24.60	649.40	833.17	724.02	0.19		
A7							
7.1	17.96	855.40	883.42	907.14	0.45	0.39	High uplift rate
7.2	16.33	727.59	753.36	765.20	0.52		
7.3	19.73	552.98	635.18	645.49	0.23		
7.4	20.17	533.93	571.19	605.38	0.37		
A8							
8.1	21.99	1062.05	1242.64	1281.68	0.11	0.23	High uplift rate
8.2	22.70	945.27	1057.80	1070.13	0.19		
8.3	16.99	773.70	892.72	878.50	0.15		
8.4	10.99	600.04	660.87	726.31	0.12		
8.5	27.32	946.65	1030.28	1077.65	0.25		
8.6	9.80	868.69	888.85	884.66	0.54		
A9							
9.1	17.80	622.58	690.87	675.56	0.29	0.36	High uplift rate
9.2	13.38	837.53	862.08	866.66	0.50		
9.3	14.72	654.30	708.70	706.23	0.28		
A10							
10.1	12.55	841.83	889.74	879.67	0.29	0.23	High uplift rate
10.2	10.64	821.66	871.67	867.88	0.22		
10.3	10.41	697.49	755.29	763.35	0.17		
10.4	22.71	600.05	711.59	665.20	0.26		
A11							
11.1	10.65	753.33	776.52	777.81	0.45	0.34	High uplift rate
11.2	12.30	814.64	838.24	831.05	0.61		
11.3	8.56	734.45	757.19	757.91	0.37		
11.4	11.58	766.05	786.75	805.62	0.38		
11.5	11.91	667.97	698.87	716.88	0.30		
11.6	13.26	629.34	665.83	680.61	0.30		
11.7	15.82	682.68	750.71	731.84	0.27		
11.8	9.75	718.14	738.81	742.86	0.43		

11.9	10.28	884.35	938.19	940.86	0.19	0.36	High uplift rate
11.10	12.47	917.53	989.41	1012.25	0.15		
11.11	9.84	879.82	921.45	944.23	0.19		
11.12	16.08	782.89	819.69	838.26	0.35		
11.13	14.26	794.82	837.64	823.80	0.40		
A12							
12.1	18.24	876.55	936.59	964.68	0.25	0.36	High uplift rate
12.2	14.86	826.01	910.94	876.41	0.22		
12.3	15.09	844.85	862.97	882.01	0.55		
12.4	12.30	766.13	796.24	781.28	0.54		
12.5	12.71	901.93	985.46	959.48	0.18		
12.6	5.77	718.98	730.03	733.69	0.45		
A13							
13.1	17.26	1007.82	1164.06	1075.99	0.15	0.31	High uplift rate
13.2	16.73	923.61	1051.65	1053.00	0.13		
13.3	8.55	804.14	824.70	836.02	0.33		
13.4	14.34	818.24	877.35	884.95	0.23		
13.5	25.89	781.16	970.35	848.95	0.20		
13.6	10.09	770.09	783.25	823.54	0.30		
13.7	7.64	750.26	776.58	782.40	0.26		
13.8	8.97	698.55	723.72	732.16	0.31		
13.9	14.08	655.57	700.67	674.93	0.44		
13.10	21.08	647.56	671.11	681.91	0.73		
A14							
14.1	11.98	968.21	1004.98	1001.91	0.34	0.28	High uplift rate
14.2	9.27	913.72	977.44	968.93	0.16		
14.3	10.52	792.36	863.07	879.65	0.13		
14.4	5.89	666.13	674.90	680.89	0.50		
A15							
15.1	25.74	970.03	1120.06	1023.79	0.25	0.35	High uplift rate
15.2	19.03	860.28	974.72	960.56	0.18		
15.3	22.19	775.36	983.31	820.42	0.18		
15.4	22.35	781.81	893.74	899.11	0.20		
15.5	24.92	1197.64	1294.00	1342.00	0.21		
15.6	17.30	1005.71	1098.89	1126.09	0.16		
15.7	15.07	1029.01	1099.67	1113.80	0.19		
15.8	11.46	922.62	945.05	932.64	0.71		
15.9	12.35	944.75	964.99	973.50	0.50		
15.10	11.79	992.93	1073.51	1060.06	0.16		
15.11	15.63	861.89	942.27	951.22	0.18		
15.12	22.06	882.29	959.76	952.80	0.30		
15.13	14.45	800.62	859.40	850.95	0.26		
15.14	13.63	725.72	780.47	755.94	0.32		
15.15	13.54	677.71	703.05	766.11	0.24		
15.16	12.24	865.67	876.78	894.37	0.61		
15.17	12.82	831.69	870.24	855.52	0.41		
15.18	16.93	784.63	831.50	828.44	0.37		
15.19	13.64	805.75	814.76	859.13	0.44		
15.20	11.31	710.12	743.56	772.44	0.24		
15.21	14.31	743.36	765.97	835.75	0.25		
15.22	12.45	681.69	730.83	717.70	0.29		
15.23	21.03	710.55	734.28	761.17	0.57		
15.24	11.61	772.56	794.41	810.56	0.39		
15.25	10.10	741.79	747.64	754.33	1.10		
A16							
16.1	7.65	619.88	646.96	649.07	0.27	0.45	High uplift rate
16.2	14.20	630.10	671.19	662.70	0.39		
16.3	12.88	631.87	656.75	672.27	0.39		
16.4	15.45	637.89	670.93	651.19	0.67		
16.5	9.98	644.98	665.78	672.28	0.42		
16.6	9.13	649.48	667.13	669.23	0.49		
16.7	8.82	669.05	687.11	684.01	0.53		
A17							
17.1	10.11	648.05	666.08	661.32	0.65	0.39	High uplift rate
17.2	7.41	653.36	676.03	672.56	0.35		
17.3	8.30	644.63	668.82	658.34	0.44		
17.4	12.21	668.99	704.93	705.23	0.34		
17.5	11.91	732.04	785.90	800.95	0.19		
17.6	13.87	744.63	792.23	811.58	0.24		

17.7	11.18	654.47	682.69	672.93	0.48		
17.8	8.83	648.09	670.60	670.89	0.39		
17.9	5.90	663.94	674.42	681.96	0.41		
17.10	11.51	660.60	696.69	680.56	0.41		
17.11	9.40	706.50	727.40	740.95	0.34		
A18							
18.1	10.13	659.88	688.07	689.86	0.35	0.26	High uplift rate
18.2	12.72	682.07	714.35	720.29	0.36		
18.3	10.58	693.34	724.27	730.68	0.31		
18.4	9.69	740.34	769.10	759.16	0.41		
18.5	15.52	763.48	806.67	857.70	0.23		
18.6	34.48	736.43	920.42	912.77	0.19		
18.7	13.18	715.95	771.78	743.51	0.32		
18.8	14.18	949.37	1012.79	1004.60	0.24		
18.9	11.68	964.56	1037.60	1003.99	0.21		
18.10	17.31	816.38	939.13	1001.49	0.11		
18.11	15.74	929.43	1054.10	1124.18	0.10		
A19							
19.1	13.37	729.53	785.66	767.30	0.28	0.47	High uplift rate
19.2	14.23	768.50	784.22	823.88	0.40		
19.3	20.71	676.28	726.79	688.99	0.66		
19.4	14.16	669.81	754.80	681.16	0.29		
19.5	9.07	651.79	685.05	680.81	0.29		
19.6	9.62	653.59	681.82	682.00	0.34		
19.7	14.19	654.38	682.57	678.56	0.54		
19.8	10.07	673.83	688.02	698.51	0.52		
19.9	11.81	681.67	709.84	704.73	0.46		
19.10	10.39	663.64	669.75	679.29	0.95		
A20							
20.1	13.48	850.13	946.09	962.13	0.13	0.20	High uplift rate
20.2	12.09	849.80	926.14	915.57	0.17		
20.3	12.78	846.18	922.97	910.38	0.18		
20.4	26.67	797.60	928.20	905.80	0.22		
20.5	16.01	820.58	911.02	918.59	0.17		
20.6	16.23	810.86	906.21	1004.38	0.11		
20.7	17.49	839.62	943.02	999.57	0.13		
20.8	13.20	717.37	776.73	748.73	0.29		
20.9	18.18	715.08	794.09	806.55	0.21		
20.10	14.25	756.67	824.20	808.24	0.24		
20.11	20.93	680.20	785.73	743.25	0.25		
20.12	19.64	701.58	768.86	854.32	0.18		
20.13	21.11	785.40	893.41	998.30	0.13		
20.14	10.30	764.45	881.85	849.61	0.10		
20.15	11.57	788.64	834.93	846.64	0.22		
20.16	12.04	758.82	855.04	833.66	0.14		
20.17	9.86	769.63	839.50	806.46	0.18		
20.18	12.32	787.39	869.14	840.81	0.18		
20.19	14.67	728.94	786.97	791.45	0.24		
20.20	28.25	730.68	873.00	847.69	0.22		
20.21	15.70	815.20	877.28	940.94	0.17		
20.22	7.69	1037.44	1051.51	1068.22	0.34		
20.23	16.33	913.04	1013.41	961.86	0.22		
20.24	24.07	843.06	937.20	955.51	0.23		
20.25	13.39	1021.51	1079.76	1057.53	0.28		
A21							
21.1	18.00	817.30	908.95	890.20	0.22	0.18	High uplift rate
21.2	22.81	724.48	824.21	873.15	0.18		
21.3	14.11	563.77	755.50	810.96	0.06		
21.4	23.15	502.89	776.87	856.42	0.07		
21.5	17.06	659.53	841.61	856.44	0.09		
21.6	16.19	834.93	915.12	953.97	0.16		
21.7	28.67	663.46	811.17	917.47	0.14		
21.8	30.16	800.68	951.32	951.32	0.20		
21.9	19.94	840.99	1006.59	946.31	0.15		
21.10	24.77	781.20	918.74	883.56	0.21		
21.11	18.60	1240.15	1275.59	1284.80	0.46		
A22							
22.1	17.33	540.58	721.77	672.00	0.11	0.14	High uplift
22.2	17.56	695.84	965.99	756.32	0.11		

22.3	17.45	374.60	602.60	530.57	0.09		rate
22.4	23.30	572.90	789.42	822.74	0.10		
22.5	14.96	685.36	874.27	852.14	0.08		
22.6	19.05	908.20	994.94	999.53	0.21		
22.7	17.75	898.15	1034.28	970.77	0.17		
22.8	15.95	770.24	889.23	882.77	0.14		
22.9	21.76	713.19	805.69	848.14	0.19		
22.10	22.72	645.04	770.70	765.46	0.18		

I. Geomorphic Index Drainage Density (Dd)

Drainage density analysis on twenty-two sub-watersheds has value ranging 2.73 – 7.29 Km⁻¹ with landform texture category ranging are rough – very smooth (Table 4). The highest Dd value is very smooth landform texture on A16 sub-watershed then smooth texture only on A9 sub-watershed. Slightly smooth texture found on seven sub-watershed and moderate texture on twelve sub-watersheds, while rough texture found only on A14 sub-watershed (Fig.11).

TABLE 4. Drainage Density (Dd) calculation results in research area.

Sub-Water shed	Area (Km ²)	Total Length River (Km)	Dd (Km ⁻¹)	Landform Texture
A1	11.29	32.84	2.91	Moderate
A2	29.47	121.29	4.12	Moderate
A3	8.36	36.61	4.38	Slightly Smooth
A4	43.52	148.54	3.41	Moderate
A5	8.63	37.76	4.38	Slightly Smooth
A6	48.21	176.29	3.66	Moderate
A7	9.19	33.83	3.68	Moderate
A8	27.27	145.79	5.35	Slightly Smooth
A9	3.27	19.90	6.09	Smooth
A10	8.55	28.11	3.29	Moderate
A11	11.61	48.19	4.15	Slightly Smooth
A12	11.33	40.02	3.53	Moderate
A13	8.74	28.83	3.30	Moderate
A14	4.24	11.59	2.73	Rough
A15	34.37	129.46	3.77	Moderate
A16	2.08	15.13	7.29	Very Smooth
A17	11.77	50.48	4.29	Slightly Smooth
A18	8.55	30.25	3.54	Moderate
A19	2.53	9.25	3.66	Moderate
A20	35.15	146.51	4.17	Slightly Smooth
A21	19.67	73.55	3.74	Moderate
A22	17.77	74.07	4.17	Slightly Smooth

The hot spring appears on A2 (Dd; 4.12 Km), A6 (Dd; 3.66) and A15 (Dd; 3.77 Km) sub-watershed with moderate class of drainage density represented by orange color. The A15 sub-watershed located on area that arranged of alluvium and sediment lake deposit Quarter rock unit (Nurhadi et al., 2009). A2 sub-watershed located on area arranged of volcanic Tertiary rocks unit, and A6 sub-watershed arranged by two type of rock unit while the hot spring located on sediment and metasediment Quarter rock unit (Rock et al.,1983). The appearance of hot spring is interpreted affected by moderate permeability and density rock, also affected by geological activity such as tectonic, erosion, and weathering.

J. Geomorphic Indices Characterization Related to Manifestation Appearance in Research Area

Main lineament geological pattern analysis and regional geologic show an orientation tendency northwest – southeast (NW – SE). The lineament that interpreted as fault deformed

the rocks and form a weak zone (permeable) as a path flow for sub-surface fluids come out to the surface. The hot springs distribution also shows a tendency with northwest – southeast

(NW – SE) orientation, interpreted that the distribution is influenced by geological lineament pattern (fault).

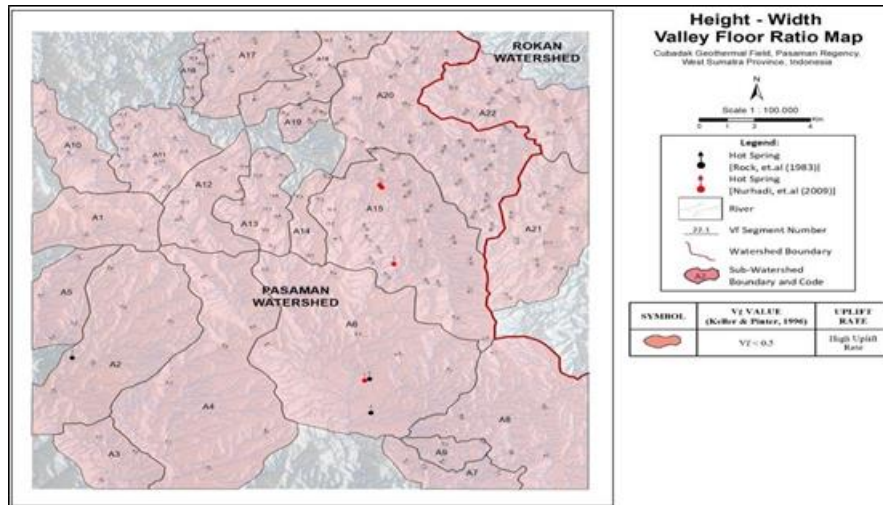


Fig 10. Valley Floor Width – Valley Height Ratio (Vf) map show all of research area has high uplift tectonic rate.

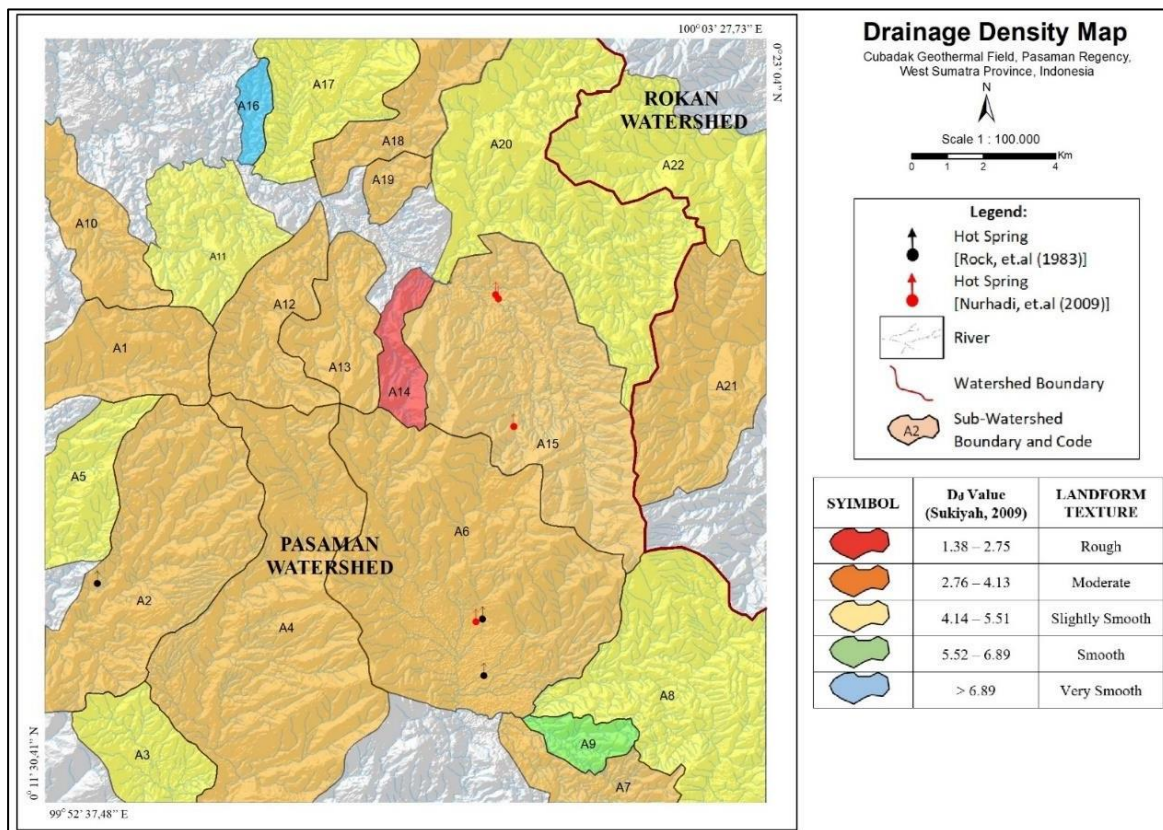


Fig 11. Drainage Density (Dd) map show that research area has five class of landform texture (rough – very smooth).

Geomorphic indices analysis results the hot spring appears on area with low – moderate of lineament density (Ld) value and active – moderate tectonic activity of sinuosity mount front (Smf) value. Analysis of Rb, Vf and Dd index show that all of hot springs appears on area with high uplift rate (Vf), not deformed area (Rb) and moderate landform texture (Dd). Based on geomorphic indices analysis the hot spring classified into

three groups and then correlated to the geologic, geochemistry and geophysics condition (Table 5 and Fig 12).

- a) **AR1 manifestation group:** Located on depression area in A6 and A15 sub-watershed, low lineament density class (Ld; $0.000 - 0.468 \text{ Km}^{-1}$), active tectonic (Smf; 1.3 – 1.6), high uplift rate (Vf; 1.9 – 0.35), not deformed area (Rb; 3.64 – 3.85) and moderate landform texture (Dd; 3.66 – 3.77

Km⁻¹). Geologically the northern part of this group located on alluvium Quarter unit rock and the southern part located on alluvium Holocene unit rock. Geochemistry data show the northern area have chloride – bicarbonate water type in partial equilibrium – immature water state, while the southern area have bicarbonate water type in immature water state. Geophysics data show the northern area have alteration zone in 100 – 500 meter depth.

b) **AR2 manifestation group:** Located on high-rise area in A15 sub-watershed, moderate lineament density class (Ld; 0.468 – 0.806 Km⁻¹), active tectonic (Smf; 1.5), high uplift rate (Vf; 0.35), not deformed area (Rb; 3.64) and moderate landform texture (Dd; 3.77 Km⁻¹). Geologically this group

located on area that arranged of sediment lake deposit Quarter rock unit. Geochemistry data show bicarbonate water type in immature water state. This group have alteration zone in 100 - 750 meter depth base on geophysics data.

c) **AR3 manifestation group:** Located on high-rise area in A2 sub-watershed, moderate lineament density class (Ld; 0.468 – 0.806 Km⁻¹), moderate tectonic activity (Smf; 2.2), high uplift rate (Vf; 0.20), not deformed area (Rb; 3.67) and moderate landform texture (Dd; 4.12 Km⁻¹). Geologically this group located on area that arranged of volcanic Miocene rock unit.

TABLE 5. Hot spring groups based on geomorphic indices characterization and correlated to geologic, geochemistry and geophysics data.

Index	HOT SPRING GROUP		
	AR 1	AR 2	AR 3
Location	Depression area	High-rise area	High-rise area
Ld (Lineament Density)	Low (Ld; 0 – 0.468 Km ⁻¹)	Moderate (Ld; 0.468 – 0.806 Km ⁻¹)	Moderate (Ld; 0.468 – 0.806 Km ⁻¹)
Smf (Mount Front Sinuosity)	Active Tectonic (Smf; 1.3 – 1.6)	Active Tectonic (Smf; 1.5)	Moderate Active Tectonic (Smf; 2.2)
Vf (Valley Floor Width – Valley Height Ratio)	High Uplift Tectonic Rate (Vf; 0.19 – 0.35)	High Uplift Tectonic Rate (Vf; 0.35)	High Uplift Tectonic Rate (Vf; 0.2)
Rb (Bifurcation Ratio)	Not Deformed (Rb; 3.64 – 3.85)	Not Deformed (Rb; 3.64)	Not Deformed (Rb; 3.67)
Dd (Drainage Density)	Moderate (Dd; 3.66 – 3.77 Km ⁻¹)	Moderate (Dd; 3.77 Km ⁻¹)	Moderate (Dd; 4.12 Km ⁻¹)
Sub-Watershed	A6 and A15 (Pasaman Watershed)	A15 (Pasaman Watershed)	A2 (Pasaman Watershed)
Geologic Data (Rock et al., 1983; Nurhadi et al., 2009)	North: Quarter alluvium rock South: Holocene alluvium rock	Quarter sediment lake deposits	Miocene Volcanic Tuff
Geochemistry Data (Nurhadi et al., 2009; Joni and Rahadinata, 2017; Utami et al., 2018)	North: chloride – bicarbonate water type in partial equilibrium – immature water state South: Bicarbonate water and immature water state	Bicarbonate water type in immature water state	None
Geophysics Data (Syahwanti et al., 2016; Joni and Rahadinata, 2017)	Alteration zone in 100 – 500 m depth occupies in the northern part of research area at A15 subwatershed	Alteration zone in 100 – 750 m occupies in the central part of research area at A15 subwatershed	None

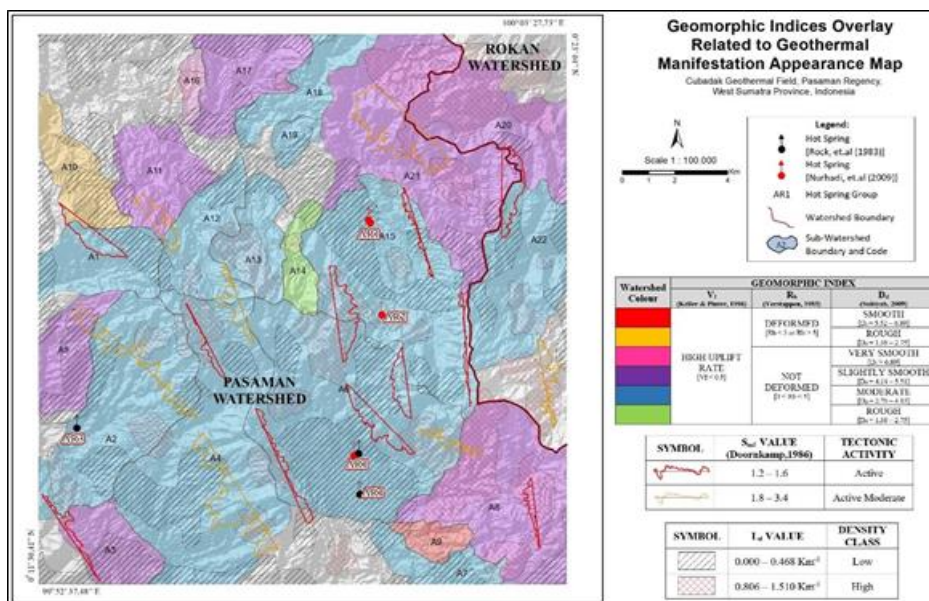


Fig 12. Overlays map of five geomorphic indices; lineament density (Ld), mount front sinuosity (Smf), bifurcation ratio (Rb), valley floor width – valley height ratio (Vf), and drainage density (Dd) show the appearance of geothermal manifestation located on area with low – moderate lineament density, moderate - activetectonic activity, not deformed area, high uplift tectonic rate, and moderate landform texture.

IV. CONCLUSION

Based on geological lineament and five geomorphic indices analysis (Ld, Smf, Rb, Vf and Dd) on SRTM-DEM map and SHP data, it can be concluded:

1. Main lineament pattern that associated with geological structure of research area have relatively northwest – southeast (NW – SE) orientation. This pattern has the same orientation with Sumatra Fault System (SFS). The analysis also has lineament with northeast – southwest (NE – SW) orientation interpreted as minor lineament. The appearance and distribution of hot springs is controlled by lineament pattern (geological structure) that showed by the same direction of hot spring distribution with main lineament pattern.
2. Geomorphic indices analysis results rough – very smooth landform texture (Dd; 2.73 – 7.29 Km⁻¹), deformed and not deformed area (Rb; 3.26 – 6.92), high uplift rate (Vf; 0.14 – 0.47), low – high lineament density (Ld; 0.000 – 1.510 Km⁻¹) and active – moderate tectonic activity (Smf; 1.0 – 3.2).
3. The hot spring appearance analysis based on geomorphic indices classified into three group hot spring manifestation are (a) AR1: Located on depression area in A6 and A15 sub-watershed, low lineament density class, active tectonic, high uplift rate, not deformed area and moderate landform texture. (b) AR2: Located on high-rise area in A15 sub-watershed, moderate lineament density class, active tectonic, high uplift rate, not deformed area and moderate landform texture, (c) AR3: Located on high-rise area in A2 sub-watershed, moderate lineament density class, moderate tectonic activity, high uplift rate, not deformed area and moderate landform texture.

ACKNOWLEDGMENT

Thank you to Geological Engineering Faculty of Padjadjaran University and all of peoples who have supported this journal writing and publication.

REFERENCES

- [1] Adiarso, Hilmawan, E., and Sugiyono, A. 2020. Outlook Energi Indonesia 2020 Edisi Khusus: Dampak Pandemi Covid-19 Terhadap Sektor Energi di Indonesia. Jakarta: Badan Pusat Pengkajian dan Penerapan Teknologi. ISBN: 978-602-1328-14-9.
- [2] Badan Informasi Geospasial. 2015. Atlas Bentanglahan Sumatera. ISBN: 817525766-0
- [3] Badan Pusat Statistik Indonesia (BPS). 2020. Neraca Energi Indonesia 2015-2019. ISSN: 0854-7068
- [4] Bemmelen, R.W van. 1949. The Geology of Indonesia, vol. IA: General Geology of Indonesia and Adjacement Archipelagoes. The Hague: Martinus Nihhoff.
- [5] Direktorat Jendral Energi Baru Terbarukan dan Konversi Energi (Ditjen EBTKE). 2017. Potensi Panas Bumi Indonesia Jilid 1. Jakarta: Kementerian Energi dan Sumber Daya Mineral.
- [6] Direktorat Jendral Energi Baru Terbarukan dan Konversi Energi (Ditjen EBTKE). 2020. Rencana Strategis 2020-2024. Jakarta: Kementerian Energi dan Sumber Daya Mineral.
- [7] Doornkamp, J.C. 1986. Geomorphological Approaches to The Study of Neotectonics. *Journal of Geological Society*, 143: 335-342.
- [8] El Hamdouni, R., Irigaray, C., Fernandez, T., Chacon, J., and Keller, E.A. 2008. Assesment of Relative Active Tectonics, Southwest Border of The Sierra Nevada (Southern Spain). Elsevier: *Geomorphology*. 96(1-2): 150-173
- [9] Gentana, D., Sulaksana, N., Sukiyah, E., and Yuningsih, E.T. 2018. Index of Active Tectonic Assessment: Quantitative-based Geomorphometric and Morphotectonic Analysis at Way Belu Drainage Basin, Lampung Province, Indonesia. *International Journal on Advanced Science Engineering Information Technology*, 8(6): 2460-2471.
- [10] Gentana, D. 2018. Indeks Geomorfik Sebagai Dasar Karakterisasi Neotektonik Untuk Penentuan Prospek Panasbumi di Gunung Rendingan dan Sekitarnya, Lampung. Bandung: Disertasi Program Pasca Sarjana Fakultas Teknik Geologi Universitas Padjadjaran (notpublished)
- [11] Joni, W., and Rahadinata, T. 2018. Struktur Sistem Panas Bumi Daerah Cubadak Berdasarkan Pemodelan Inversi 3-D Data Magnetotellurik. *Buletin Sumber Daya Geologi*, 13(1): 59-69.
- [12] Keller, E.A., and Pinter, N. 1996. Active Tectonics: earthquakes, uplift and landscape (2nd edition). New Jersey: Prentice Hall.
- [13] Lumbanbatu, U.M. 2009. Morfogenetik Daerah Lubuksikaping Provinsi Sumatera Barat. *Jurnal Sumber Daya Geologi*.19(2): 79-93.
- [14] Nugroho, A.R.M., Sukiyah, E., Syafri, I., and Isnaniarwardhani, V. 2020. Identification of Tectonic Deformation Using Morphometrical Analysis of Lamongan Volcano Complex. *International Journal of GEOMATE*, 19(71): 55-60. ISSN: 2186-2982.
- [15] Nurhadi, M., Widodo, S., Soetoyo, and Sulaeman, B. 2009. Penyelidikan Terpadu Daerah Panas Bumi Cubadak, Kabupaten Pasaman, Sumatera Barat. *Prosiding Hasil Kegiatan Lapangan Pusat Sumber Daya Geologi*.
- [16] Perez-Pena, J.V., Azor, A., Azanon, J.M., and Keller, E.A. 2010. Active Tectonics in The Sierra Nevada (Betic Cordillera, SE Spain): Insights form Geomorphic Indexes and Drainage Pattern Analysis. Elsevier: *Geomorphology*, 119(1-2): 74-87.
- [17] Poedjoprajitno, S. 2007. Morfotektonik dan Reaktivitas Sesar Sumatra di Padangpanjang, Sumatra Barat. *Jurnal Sumber Daya Geologi* 17(3): 187-204.
- [18] Pusat Vulkanologi dan Mitigasi Bencana Geologi (PVMBG). 2017. Volcanoes Distribution in Indonesia. Kementerian Energi dan Sumber Daya Mineral
- [19] Rock, S., Aldiss, D.T., Aspden, J.A., Clarke, M.C.G., Djunuddin, A., Kartawa, W., Miswar, Thompson, S.J., and Whandoyo, R. 1983. Peta Geologi Lembar Lubuksikaping, Sumatra. Pusat Penelitian dan Pengembangan Geologi.
- [20] Soengkono, S. 1999. Analysis of Digital Topographic Data for Exploration and Assesment of Geothermal System. 21st New Zealand Geothermal Workshop.
- [21] Sukiyah, E., Sulaksana, N., and Rosana, M.F. 2012. Peran Morfotektonik DAS dalam Pengembangan Potensi Energi Mikro Hidro di Cianjur-Garut bagian Selatan. *Bionatura Jurnal Ilmu Ilmu Hayati dan Fisik*, 14(1): 1-11.
- [22] Sukiyah, E. 2017. Sistem Informasi Geografis, Konsep dan Aplikasinya dalam Analisis Gemorfologi Kuantitatif Edisi 1. Bandung: Unpad Press.
- [23] Soetoyo. 2008. Hubungan Struktur Sesar dengan Terbentuknya Endapan Aliran Piroklastik di Daerah Panas Bumi Sampuraga, Madailing Natal – Sumatera Utara. *Buletin Sumber Daya Geologi*. 3(1): 2-12.
- [24] Syahwanti, H., Srigutomo, W., and Kholid, M. 2016. 2-D Resistivity Structure of Cubadak Geothermal Area Revealed from Magnetotelluric Data. *IOP Conference Series: Earth and Environmental Science*, 62.
- [25] Utami, Z.D., Putra, A., Syafitri, dan Dhia, H. 2019. The estimation of geothermal reservoir temperature using geothermometer equation in Cubadak area, Pasaman regency, West Sumatra, Indonesia. *Jurnal of Physics: Conference Series* 1185 012018.